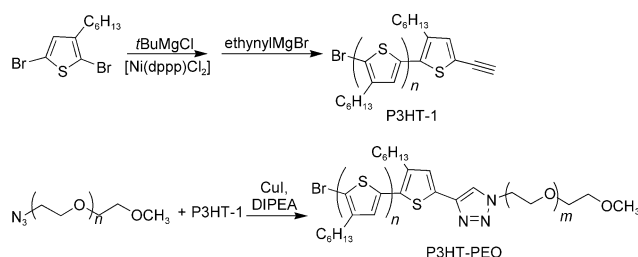


# Simultaneous Electronic and Ionic Conduction in a Block Copolymer: Application in Lithium Battery Electrodes\*\*

Anna E. Javier, Shrayesh N. Patel, Daniel T. Hallinan Jr., Venkat Srinivasan, and Nitash P. Balsara\*

Conjugated polymers such as poly(3-hexylthiophene) (P3HT) have been used extensively as the active material in various electronic devices such as solar cells,<sup>[1]</sup> field-effect transistors,<sup>[2]</sup> and light-emitting diodes.<sup>[3]</sup> Coupling these conjugated polymers to ionic conductors allows use of the polymers in electrochemical energy storage devices, which require the transport of both ions and electronic charge. The need for developing new materials for electrochemical energy storage in the emerging energy landscape, which includes electric cars and renewable stationary energy, is now widely recognized.<sup>[4]</sup> We report herein the synthesis and characterization of poly(3-hexylthiophene)-*b*-poly(ethylene oxide) (P3HT-PEO). Lithium batteries composed of a cathode with LiFePO<sub>4</sub> particles dispersed in a P3HT-PEO matrix, a solid polymer electrolyte, and lithium metal anodes were assembled. In contrast to current lithium battery electrodes, which require an inert polymer to bind the cathode particles, carbon additives for electronic conduction and a liquid electrolyte for lithium ion conduction, our system uses one material that serves as the binder and transporter of electronic charge and lithium ions.

Scheme 1 shows the synthesis of P3HT-PEO. Grignard metathesis (GRIM) polymerization was used to produce an ethynyl-terminated, regioregular P3HT (P3HT-1).<sup>[5]</sup> Regioregular P3HT forms well-defined, nanostructured polymers, while the ethynyl functional group is required for the next step. The 1,3-dipolar cycloaddition “click” reaction<sup>[6]</sup> was used to couple P3HT-1 to a commercially available, azide-terminated PEO, and was performed in the presence of CuI and diisopropylethylamine (DIPEA) in THF for 72 h at 40 °C<sup>[7]</sup> to



**Scheme 1.** Synthesis of P3HT-PEO block copolymer. dppp = 1,3-bis(diphenylphosphino)propane.

result in P3HT-PEO (detailed experimental procedures and polymer characterization (Figures S1 and S2) are shown in the Supporting Information).

Tapping-mode AFM phase images of P3HT-1 homopolymer and the P3HT-PEO copolymer thin films are shown in Figure 1a and Figure 1b, respectively. Both images show the nanofibrillar morphology that is usually reported for P3HT and its derivatives, which results from the  $\pi$ - $\pi$  stacking of the well-defined P3HT chains.<sup>[8]</sup> Both samples have nanofibril widths of approximately 20 nm, which are consistent with reported values.<sup>[9]</sup> The P3HT-1 nanofibrils appear to have a very compact arrangement with relatively little phase varia-

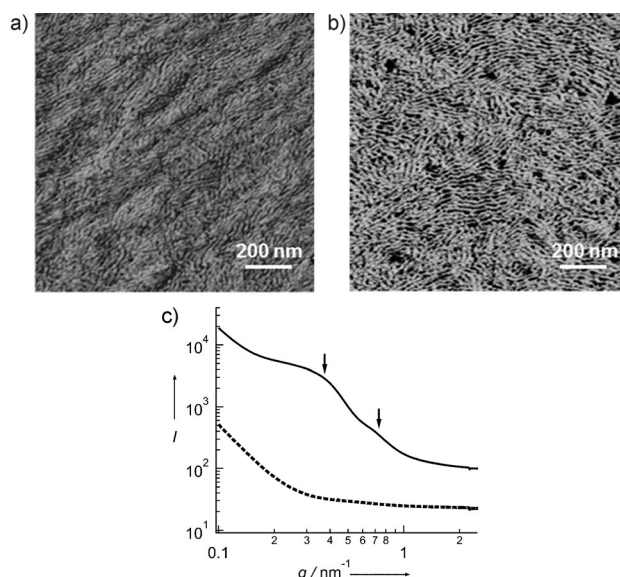


**Figure 1.** Tapping-mode AFM phase image of a) P3HT homopolymer and b) P3HT-PEO; c) SAXS profiles of neat P3HT-PEO and P3HT-PEO/LiTFSI mixture at 100 °C. — with LiTFSI; ---- neat.

[\*] Dr. A. E. Javier, Dr. D. T. Hallinan Jr., Dr. V. Srinivasan, Prof. N. P. Balsara  
Environmental Energy Technologies Division  
Lawrence Berkeley National Laboratory (LBNL)  
Berkeley, CA 94720 (USA)  
E-mail: nbalsara@berkeley.edu

Dr. A. E. Javier, S. N. Patel, Dr. D. T. Hallinan Jr., Prof. N. P. Balsara  
Department of Chemical Engineering  
University of California at Berkeley  
Berkeley, CA 94720 (USA)

[\*\*] This work was supported by U.S. DOE contract no. DE-AC02-05CH11231 BATT Program (A.E.J., D.T.H., V.S., N.P.B.), and through the LBNL LDRD Program (S.N.P., 2007–2010). S.N.P. thanks NSF (CBET 0966632). SAXS experiments were performed at the Advanced Light Source, LBNL, a DOE national user facility supported by the DOE under the same contract. We also wish to thank Profs. R.A. Segalman and M. Jeffries-EL, and Drs. H. Gao and T. Constantin for helpful discussions.

Supporting information for this article is available on the WWW under <http://dx.doi.org/10.1002/anie.201102953>.

tion (Figure 1a). In contrast, the nanofibrils in the block copolymer AFM image are separated by distinct dark regions (Figure 1b), which could indicate the location of the PEO block. These observations are consistent with previously reported data on P3HT-containing block copolymer thin films.<sup>[10]</sup> Figure 1c shows small-angle X-ray scattering (SAXS) profiles obtained from bulk samples of both neat P3HT-PEO and a P3HT-PEO/lithium salt mixture. Lithium salts are typically added to PEO to enhance its ability to solvate and conduct lithium ions. Lithium bis(trifluoromethane sulfone)-imide (LiTFSI) was added to P3HT-PEO by using procedures outlined in the Supporting Information. The molar ratio  $r$  of lithium to ethylene oxide moieties was fixed at 0.085 throughout this work. The P3HT-PEO/LiTFSI mixture shows a broad shoulder at a scattering vector  $q = 0.37 \text{ nm}^{-1}$ , and an additional, weaker shoulder at  $q = 0.74 \text{ nm}^{-1}$ , which indicate a periodic structure with a length scale of approximately 17 nm. In contrast, SAXS profiles from a bulk sample of neat P3HT-PEO contained no discernable features (Figure 1c), as expected. Whilst the AFM images showed nanostructure formation on the surface of the thin films, it is more difficult to see ordering in bulk samples of P3HT when using SAXS. In previous studies on mixtures of LiTFSI and other PEO-containing block copolymers, it was shown that the addition of the salt enhances microphase separation because of the preferential segregation of salts in the PEO block.<sup>[11]</sup> A similar effect is observed in the P3HT-PEO/LiTFSI system and gives rise to periodic structures in the SAXS profile.

The ionic and electronic conductivities of the block copolymer were determined by impedance spectroscopy and DC measurements on the P3HT-PEO/LiTFSI mixture sandwiched between two nickel electrodes. The  $Z''$  (imaginary impedance) versus  $Z'$  (real impedance) Nyquist plot contains three “semicircles” as shown in Figure 2. This result differs significantly from Nyquist plots reported for pure electronic and ionic conductors, which exhibit a single semicircle.<sup>[12]</sup> Steady-state current densities, obtained under small applied dc potentials, were measured and found to be consistent with Ohm's law, and gave a resistance value of  $3.78 \text{ k}\Omega \text{ cm}^2$  (Figure 2, right-hand inset). This value is approximately equal to the sum of the diameters of all three Nyquist semicircles ( $R_3$ ) shown in Figure 2. Since nickel is a blocking electrode for lithium ions, the dc experiments must reflect the electronic resistance,  $R_e$ , of the sample. The equivalent circuit shown in the left-hand inset in Figure 2 is the simplest circuit that can be constructed based on the impedance data. A similar circuit with two semicircles was proposed for mixed conduction in amorphous poly(*p*-phenylene) homopolymers.<sup>[13]</sup> The elements shown in blue in Figure 2 are necessary for fitting our experimental data and include capacitance,  $Q_g$ , and resistance,  $R_g$ , which were previously used to describe transport across grain boundaries in impedance data obtained from inorganic mixed conductors.<sup>[12a]</sup> It is not clear if this explanation is applicable to our system. The ionic resistance,  $R_i$ , can be determined from the relationship  $R_i = (R_3 R_1)/(R_3 - R_1)$ , where  $R_1$  is the high-frequency semi-circle resistance. The conductivity is given by  $\sigma = L/R$ , where  $L$  is the polymer thickness and  $R$  is the resistance. We thus obtain the ionic conductivity,  $\sigma_i$ , as  $(1.09 \pm 0.469) \times 10^{-4} \text{ S cm}^{-1}$  and

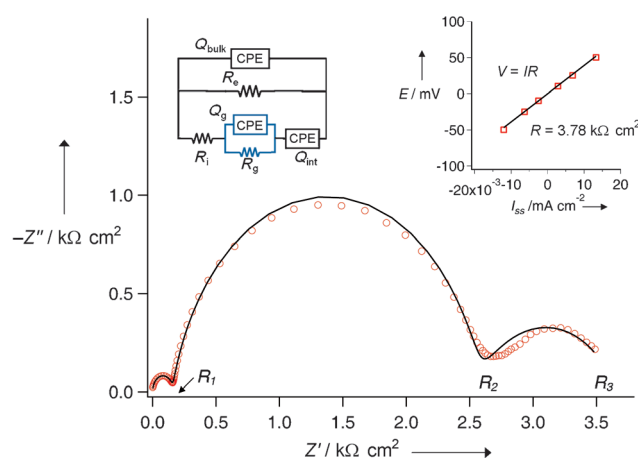


**Figure 2.** Conductivity measurements. Nyquist plot of the P3HT-PEO/LiTFSI mixture sandwiched between nickel electrodes ( $-Z''$  (imaginary) vs  $Z'$  (real) impedance). Red circles correspond to experimental data and the black curve corresponds to a fit using the proposed equivalent circuit comprising resistors and constant phase elements (CPE) shown in the left-hand inset. The right-hand inset shows the Ohm's law fit of dc potentials ( $E$ , applied potential) vs steady-state current density ( $I_{ss}$ ).  $R_1$ ,  $R_2$ , and  $R_3$  correspond to the resistance values of each semicircle relative to the origin.  $Q_{bulk}$  = bulk capacitance,  $Q_{int}$  = interfacial capacitance. See the Supporting Information for more details.

the electronic conductivity,  $\sigma_e$ , as  $(6.73 \pm 0.05) \times 10^{-6} \text{ S cm}^{-1}$ , which are consistent with the reported values (note that  $\sigma_e$  is the electronic conductivity of pristine, unoxidized P3HT).<sup>[14]</sup> A full fit of the data using the equivalent circuit in Figure 2 gives  $R_i$  and  $R_e$  values that are within experimental error (see the Supporting Information for details). Current models<sup>[15]</sup> indicate that the performance of battery electrodes are dependent only on  $R_i$  and  $R_e$  values, and not on other parameters contained in the equivalent circuit.

After showing that the polymer exhibits simultaneous ionic and electronic conductivity, the polymer was used as matrix material in a  $\text{LiFePO}_4$  battery cathode. The cathode film was prepared by dissolving P3HT-PEO and LiTFSI in THF, then adding  $\text{LiFePO}_4$  particles to the solution and homogenizing for approximately 5 min. The mixture was cast on aluminum foil, and doctor-bladed to obtain a smooth film. The film was dried overnight under vacuum at  $70^\circ\text{C}$ . All processing steps were performed inside a glove box under an Ar atmosphere. All cathodes used in this study contained 50 wt %  $\text{LiFePO}_4$ . Figure 3a shows an SEM image of the film obtained from the  $\text{LiFePO}_4$ /P3HT-PEO/LiTFSI mixture. The

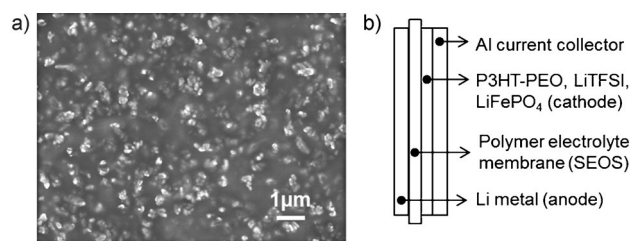


**Figure 3.** a) SEM image of the cathode composed of P3HT-PEO/LiTFSI and  $\text{LiFePO}_4$ ; b) schematic of the battery construction.

$\text{LiFePO}_4$  particles appear as bright spots and the polymer/salt mixture appears as a dark matrix. This film is remarkably simple when compared to a traditional lithium ion cathode, which contains pores for ionic conduction, conductive carbon additives for electronic conduction, and an inert polymeric binder to hold the structure in place, in addition to the active material. In our system, the active material is dispersed in a single polymer that functions simultaneously as the conductor of lithium ions and electronic charge, as well as binder material in the cathode.

A schematic of the battery cross-section is given in Figure 3b. To assemble a battery cell, a  $1\text{ cm}^2$  circular cathode was punched out of the cast film and pressed onto a  $30\text{--}50\text{ }\mu\text{m}$  thick film made from a mixture of polystyrene-*b*-poly(ethylene oxide)-*b*-polystyrene (SEOS)/LiTFSI (see the Supporting Information for more details on the SEOS synthesis). The SEOS/LiTFSI film serves as a solid polymer electrolyte membrane (Figure 3b), and a piece of lithium pressed onto the other side of the membrane completes the cell. Several cells were then cycled from  $3.8\text{ V}$  to  $2.5\text{ V}$  at a constant current density of  $0.02\text{ mA cm}^{-2}$ . This current translates to a 4 h symmetric charge–discharge cycle with a 1 h rest step between each charge and discharge run. The average specific capacities of ten batteries obtained during the first ten cycles are shown in Figure 4a, and sample charge and discharge cycles are shown in Figure 4b. The batteries show a specific capacity that approaches the theoretical value for  $\text{LiFePO}_4$  ( $170\text{ mAh g}^{-1}$ ) with relatively little capacity fade. This result provides further evidence that the P3HT-PEO copolymer delivers both ions and electronic charge to the active centers, thus allowing the batteries to cycle efficiently.

An important factor is that P3HT is a semiconductor, and its conductivity can be dramatically altered by oxidation or doping. It is known that the conductivity of poly(3-alkylthiophenes) increases by several orders of magnitude upon exposure to oxidizing chemicals such as iodine,<sup>[8]</sup> or when applying potentials of approximately  $3.2\text{ V}$  relative to  $\text{Li}^+/\text{Li}$ .<sup>[16]</sup> Results of cyclic voltammetry experiments (Figure 4c) confirm that this behavior is also valid for the P3HT-PEO copolymer, where the onset of oxidation occurs at around  $3.1\text{ V}$ . It is thus clear that electrochemical doping of the P3HT block arises from the applied potentials during the charge–discharge cycles and enhances electronic transport over and above that obtained in the undoped state (Figure 2). Two sets of impedance spectra of the entire battery taken during consecutive cycles are shown (Figure 4b, inset). One set of spectra was measured at the end of the charge cycle (a,b,c,d), the second set measured at the end of the discharge cycle (e,f,g). The overall resistance of the entire cell changes by an order of magnitude when going from a fully charged to fully discharged state, and the change is reversible from one cycle to the next. The possibility of changing the electronic resistance of the battery in situ offers unprecedented possibilities for control. For example, the bandgap of the electronically conducting block can, in principle, be engineered to enable properties such as rapid charging and overcharge/overdischarge protection.

To summarize, a P3HT-PEO block copolymer that exhibits simultaneous ionic and electronic conductivity was

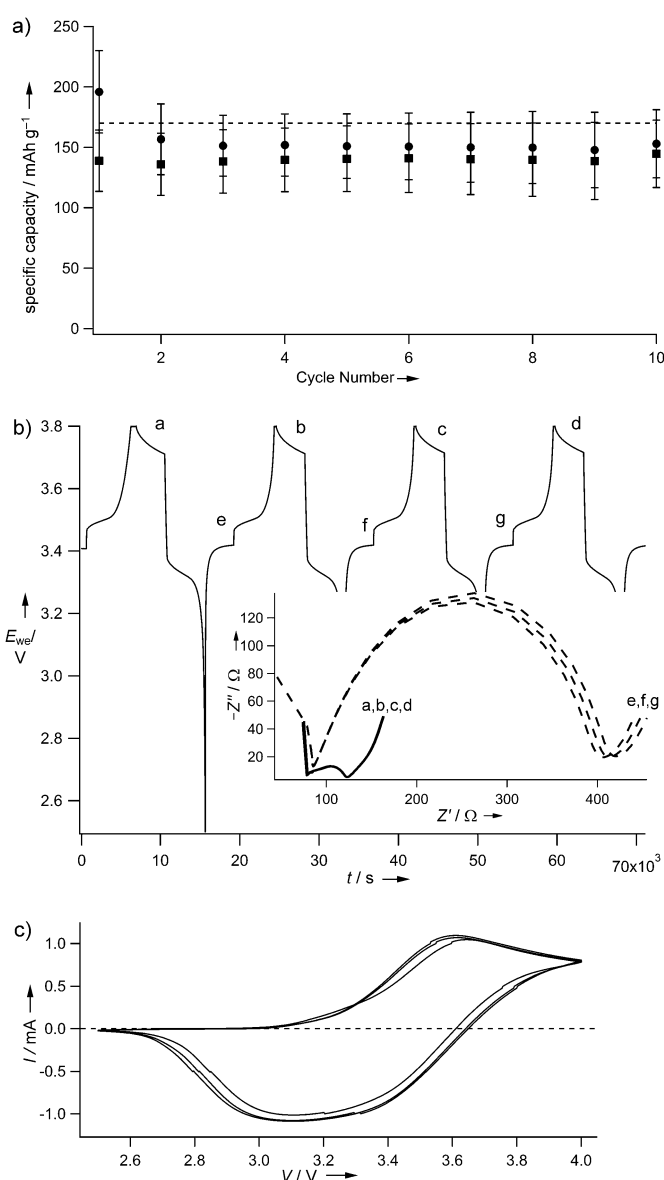


**Figure 4.** Battery cycling data. a) Average specific capacity ( $\text{mAh g}^{-1}$ ) for 10 cells as a function of cycle number (● charge; ■ discharge; ---- theoretical specific capacity of  $\text{LiFePO}_4$ ); b) cycling plot (cell potential  $E_{we}$  vs time) of a battery composed of a lithium anode, a solid electrolyte, and a P3HT-PEO/ $\text{LiFePO}_4$  cathode. Inset: Nyquist impedance plots taken at specified points after charging (a–d) and discharging (e–g) the battery; c) cyclic voltammogram of P3HT-PEO using SEOS/LiTFSI as solid electrolyte and Li foil as both counter- and reference electrodes (scanned from  $2.5\text{--}4.0\text{ V}$  vs  $\text{Li}^+/\text{Li}$ , scan rate of  $20\text{ mV s}^{-1}$ ).

synthesized and characterized by a combination of ac impedance, dc polarization, AFM, and SAXS measurements. It was found that the addition of a lithium salt increases microphase separation and enhances the ordering in P3HT-PEO bulk samples. The polymer was used in a battery cathode, and cycling experiments demonstrated that P3HT-PEO delivers both ions and electronic charge to the active centers. All of the supporting functions required in a battery electrode are thus performed by a single material. The

presence of a semiconductor in the electrode can enable the design of responsive electrodes.

Received: April 29, 2011

Revised: July 15, 2011

Published online: September 7, 2011

**Keywords:** block copolymers · click chemistry · conducting materials · electrochemistry · nanostructures

- [1] P. C. Ewbank, D. Laird, R. D. McCullough in *Organic Photovoltaics* (Eds.: C. Brabec, V. Dyakonov, U. Scherf), Wiley-VCH, **2009**, pp. 1–55.
- [2] H. Sirringhaus in *Organic Field-Effect Transistors* (Eds.: Z. Bao, J. Locklin), CRC Press, **2007**, pp. 103–137.
- [3] K. Mullen, U. Scherf, *Organic Light Emitting Devices: Synthesis Properties, and Applications*, Wiley-VCH, Weinheim, Germany, **2006**.
- [4] M. Armand, J. M. Tarascon, *Nature* **2008**, *451*, 652–657.
- [5] a) R. S. Loewe, S. M. Khersonsky, R. D. McCullough, *Adv. Mater.* **1999**, *11*, 250–253; b) M. Jeffries-El, G. Sauve, R. D. McCullough, *Macromolecules* **2005**, *38*, 10346–10352.
- [6] a) H. C. Kolb, M. G. Finn, K. B. Sharpless, *Angew. Chem.* **2001**, *113*, 2056–2075; *Angew. Chem. Int. Ed.* **2001**, *40*, 2004–2021; b) J.-F. Lutz, *Angew. Chem.* **2007**, *119*, 1036–1043; *Angew. Chem. Int. Ed.* **2007**, *46*, 1018–1025.
- [7] T. L. Benanti, A. Kalaydjian, D. Venkataraman, *Macromolecules* **2008**, *41*, 8312–8315.
- [8] R. D. McCullough, S. Tristram-Nagle, S. P. Williams, R. D. Lowe, M. Jayaraman, *J. Am. Chem. Soc.* **1993**, *115*, 4910–4911.
- [9] R. Zhang, B. Li, M. C. Iovu, M. Jeffries-El, G. Sauve, J. Cooper, S. J. Jia, S. Tristram-Nagle, D. M. Smilgies, D. N. Lambeth, R. D. McCullough, T. Kowalewski, *J. Am. Chem. Soc.* **2006**, *128*, 3480–3481.
- [10] J. S. Liu, E. Sheina, T. Kowalewski, R. D. McCullough, *Angew. Chem.* **2002**, *114*, 339–342; *Angew. Chem. Int. Ed.* **2002**, *41*, 329–332.
- [11] a) N. S. Wanakule, J. M. Virgili, A. A. Teran, Z.-G. Wang, N. P. Balsara, *Macromolecules* **2010**, *43*, 8282–8289; b) Z.-G. Wang, *J. Phys. Chem. B* **2008**, *112*, 16205–16213.
- [12] a) R. A. Huggins, *Ionics* **2002**, *8*, 300–313; b) J. R. Maccallum, C. A. Vincent, *Polymer Electrolyte Reviews, Vol. 1*, Elsevier Applied Science Publishers Ltd., New York, **1987**; c) J. Jamnik, J. Maier, *J. Electrochem. Soc.* **1999**, *146*, 4183–4188.
- [13] J. Plochanski, H. Wycislik, *Solid State Ionics* **2000**, *127*, 337–344.
- [14] a) A. Panday, S. Mullin, E. D. Gomez, N. Wanakule, V. L. Chen, A. Hexemer, J. Pople, N. P. Balsara, *Macromolecules* **2009**, *42*, 4632–4637; b) T.-A. Chen, X. Wu, R. D. Rieke, *J. Am. Chem. Soc.* **1995**, *117*, 233–244.
- [15] J. S. Newman, K. E. Thomas-Alyea, *Electrochemical Systems*, 3rd ed., Prentice-Hall, Inc., Englewood Cliffs, N.J., **2004**.
- [16] G. Chen, T. J. Richardson, *Electrochem. Solid-State Lett.* **2004**, *7*, A23–A26.